

RESEARCH ARTICLE | AUGUST 23 2023

## Tight bounds correlating peak absorption with Q-factor in composites and metallic clusters of particles

Special Collection: **Fundamentals and Applications of Metamaterials: Breaking the Limits**

Kshiteej J. Deshmukh   ; Graeme W. Milton 

 Check for updates

*Appl. Phys. Lett.* 123, 081703 (2023)

<https://doi.org/10.1063/5.0155092>

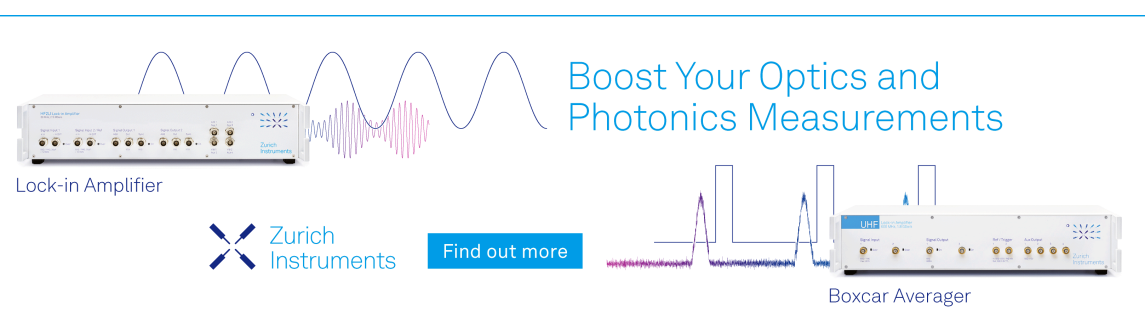


View  
Online



Export  
Citation

CrossMark



Boost Your Optics and Photonics Measurements

Lock-in Amplifier

Zurich Instruments

Find out more

Boxcar Averager

The advertisement features a blue border and two main products from Zurich Instruments. On the left, a UHF Lock-in Amplifier is shown with a sine wave and a multi-tone signal graph. On the right, a UHF Boxcar Averager is shown with a digital signal graph. The text "Boost Your Optics and Photonics Measurements" is centered above the products. The Zurich Instruments logo, featuring a stylized 'X' and the text "Zurich Instruments", is at the bottom left. A blue "Find out more" button is positioned between the two main images.

# Tight bounds correlating peak absorption with Q-factor in composites and metallic clusters of particles

EP

Cite as: Appl. Phys. Lett. **123**, 081703 (2023); doi: [10.1063/5.0155092](https://doi.org/10.1063/5.0155092)

Submitted: 18 April 2023 · Accepted: 7 August 2023 ·

Published Online: 23 August 2023



View Online



Export Citation



CrossMark

Kshiteej J. Deshmukh<sup>a)</sup>  and Graeme W. Milton 

## AFFILIATIONS

Department of Mathematics, University of Utah, Salt Lake City, Utah 84112, USA

Note: This paper is part of the APL Special Collection on Fundamentals and Applications of Metamaterials: Breaking the Limits.

<sup>a)</sup>Author to whom correspondence should be addressed: [kjdeshm@math.utah.edu](mailto:kjdeshm@math.utah.edu)

## ABSTRACT

Resonances are fundamentally important in the field of nano-photonics and optics. Thus, it is of great interest to know what are the limits to which they can be tuned. The bandwidth of the resonances in materials is an important feature, which is commonly characterized by using the Q-factor. We present tight bounds correlating the peak absorption with the Q-factor of two-phase quasi-static metamaterials and plasmonic resonators evaluated at a given peak frequency by introducing an alternative definition for the Q-factor in terms of the complex effective permittivity of the composite material. This composite may consist of well-separated clusters of plasmonic particles, and, thus, we obtain bounds on the response of a single cluster as governed by the polarizability. Optimal metamaterial microstructure designs achieving points on the bounds are presented. The most interesting optimal microstructure is a limiting case of doubly coated ellipsoids that attains points on the lower bound. We also obtain bounds on Q for three dimensional, isotropic, and fixed volume fraction two-phase quasi-static metamaterials and particle clusters with an isotropic polarizability. Some almost optimal isotropic microstructure geometries are identified.

Published under an exclusive license by AIP Publishing. <https://doi.org/10.1063/5.0155092>

The explosion of interest in metamaterials has been driven by the realization that their properties can break expected limits. These limits, or bounds, are based on assumptions that do not hold for the metamaterials in question. Naturally, one wants to know what these bounds are, and here, we focus on a fundamental problem: finding bounds that correlate the absorption at a peak with the metamaterial quality factor (Q-factor) in the quasi-static limit.

At the nanoscale, local plasmon resonances in metal particle clusters are of great interest due to their unique properties.<sup>1,2</sup> Resonances in materials have led to many exciting properties in nano-photonics and optics. A famous example is the “Lycurgus cup,” a fourth century Roman drinking cup made of glass with suspended fine particles of gold. The gold particle resonances at optical wavelengths cause it to appear either red or green depending on where the light shines.

A number of definitions for Q are found in the literature.<sup>3–8</sup> The two most common definitions of Q-factor in use are: one, the ratio of energy stored to energy radiated or dissipated; and, two, the ratio of center (resonance) frequency to frequency-bandwidth. Using the first definition of Q-factor, various bounds on the Q-factor of antennas have been proposed.<sup>9–16</sup>

The results of Bergman<sup>17</sup> and Milton<sup>18</sup> obtained independently in 1980 naturally imply bounds on the imaginary part of the dielectric constant of a quasistatic two-phase composite and, hence, on the absorption of the composite at fixed frequency. The question then arises as to how sharply peaked can be the absorption: can one obtain bounds that correlate the magnitude of the peak absorption with the bandwidth of frequencies where the absorption is at half height or with an alternate Q-factor?

There is an affiliated question for single or clusters of metal particles, of arbitrary shape but occupying a given volume. Bounds on the absorption, at fixed quasistatic frequencies, were obtained in 2014 by Miller *et al.*<sup>19</sup> In fact, however, bounds on the quasistatic complex polarizability of arbitrary shaped objects or clusters of them, and by inference the absorption, were obtained as far back as 1981: see Fig. 3 in Ref. 20. The bounds are corollary of the bounds of Bergman and Milton. The key observation is to consider a composite of a dilute suspension of the particle clusters. To first order in the volume fraction, the effective permittivity is determined by the complex polarizability so bounds on the first imply bounds on the second: see, in particular, Ref. 21. Similarly, bounds that correlate the peak absorption and

Q-factor in composites naturally imply bounds that correlate the peak absorption and Q-factor in resonating metal particle clusters. These bounds are also applicable when the particles themselves are microstructured, containing a composite of the metallic and void phases.

In this work, we find bounds that correlate an appropriate Q-factor with peak-loss in lossy two-phase quasi-static metamaterial resonators and identify microgeometries that achieve those bounds. We consider two-phase metamaterials with complex relative permittivity  $\epsilon_1(\omega)$  of one isotropic phase given, for example, by a Drude model or a Lorentz model, and with relative permittivity  $\epsilon_2(\omega) = \epsilon_2$  of the other isotropic phase taken to be a real constant. The effective permittivity of the metamaterial is some complex-valued function of the permittivities of the pure phases:  $\epsilon_{\text{eff}}(\omega) = \epsilon_{\text{eff}}(\epsilon_1(\omega), \epsilon_2)$ . Without loss of generality, we can rescale the dimensions and set the permittivity of the constant phase as<sup>22</sup>  $\epsilon_2 = 1$ . Considering the ambiguity associated with defining the energy stored in a lossy material,<sup>23-25</sup> we adopt the second definition for Q, i.e.,  $Q = \omega_R/\Delta\omega$ , where  $\omega_R$  is the center frequency and  $\Delta\omega$  is the bandwidth at half-height of the peak-absorption value, and refer to this definition as the conventional Q-factor,  $Q_c$ . However, to proceed with finding the bounds on Q in two-phase metamaterials, it is desirable to have an expression for Q in terms of the effective material parameters at the center frequency.

Assume that the response of a material permittivity is given by a Lorentz model,

$$\epsilon = 1 + \frac{\omega_p^2}{\omega_0^2 - \omega^2 - i\omega\gamma}, \quad (1)$$

where  $\omega_p$ ,  $\omega_0$ , and  $\gamma$  are the plasma frequency, natural frequency, and damping coefficient, respectively. We show analytically, that in the limit  $\omega_0/\gamma \gg 1$  (see, Sec. S1 and Fig. S1 for details),  $\gamma \approx \Delta\omega$ , i.e., the bandwidth is narrow compared to the center frequency, and the center frequency  $\omega_R$  approaches the natural frequency  $\omega_0$  ( $\omega_R \approx \omega_0$ ). Then, the expression for  $Q_c$  at an absorption peak can be approximated alternatively by defining a new Q-factor ( $Q_{\text{new}}$ ) in terms of the material parameters

$$Q_c \approx Q_{\text{new}} = -\frac{\omega_R}{2} [\text{Im}(\epsilon(\omega_R))]^{-1} \text{Re}\left(\frac{d\epsilon(\omega)}{d\omega}\right) \Big|_{\omega=\omega_R}. \quad (2)$$

Here,  $\text{Re}(\cdot)$  and  $\text{Im}(\cdot)$  denote the real and imaginary parts. Similarly, for clusters of metal particles,  $Q_{\text{new}}$  is given by  $Q_{\text{new}} = -\frac{\omega_R}{2} [\text{Im}(\alpha(\omega_R))]^{-1} \text{Re}\left(\frac{d\alpha(\omega)}{d\omega}\right) \Big|_{\omega=\omega_R}$ , where  $\alpha$  is the polarizability. In the case of local plasmon resonances in metal particle clusters, a somewhat similar expression for Q was obtained by Wang and Shen,<sup>2</sup> except while ours involves the effective dielectric constant, theirs involves the dielectric constant of metal particles, and, importantly, with this substitution theirs has the opposite sign. Our  $Q_{\text{new}}$  is still positive because of the anomalous dispersion at the absorption peak. Theirs involved the ratio of stored to absorbed energies, the first only known when the metal has very low absorption. Moreover, we allow for peaks generated by more than one, or even a continuum, of resonances, whereas they implicitly assume that  $\text{Im}(\epsilon)$  is less than the separation between resonances.

Expression (2) is also similar to ones for antennas with known impedance.<sup>5,6</sup> An expression for the Q-factor in systems with loss-less and high-loss components was obtained by Figotin and Welters.<sup>8</sup>

Figure 1 illustrates the good agreement between  $Q_c$  and  $Q_{\text{new}}$  for different Lorentz models with varying values of  $\gamma$  and  $\omega_0$  even for

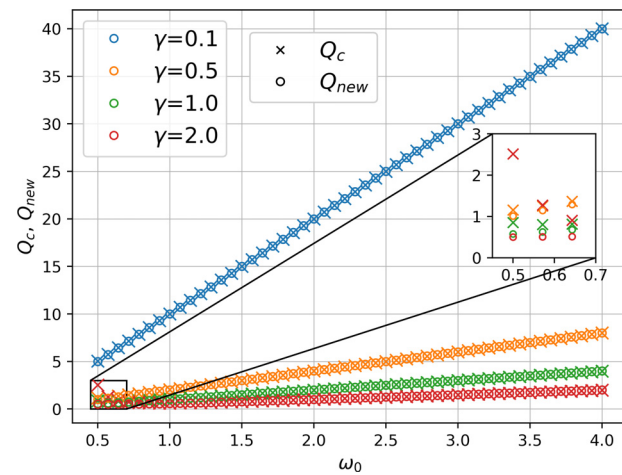


**FIG. 1.**  $Q_c$  (circle marker) vs  $Q_{\text{new}}$  (cross marker) comparison for Lorentz models with varying values of the damping coefficient  $\gamma$  and resonant frequency  $\omega_0$ . In the limits  $\omega_0/\gamma \gg 1$  and  $\omega_0/\Delta\omega \gg 1$ , we see good agreement between  $Q_c$  and  $Q_{\text{new}}$ . The inset shows the discrepancy between  $Q_c$  and  $Q_{\text{new}}$  near the origin where the approximation no longer holds.

moderately large values of  $\omega_0/\gamma$ . The zoomed inset shows that close to origin, where  $\omega_0$  is comparable to  $\gamma$  and we are well outside the validity of the approximation,  $Q_c$  and  $Q_{\text{new}}$  differ significantly.

The main idea to obtain bounds on  $Q_{\text{new}}$  in two-phase metamaterials at a given peak center frequency ( $\omega_R$ ) is to correlate, at  $\omega = \omega_R$ , the quantities  $\text{Re}(\frac{d\epsilon_{\text{eff}}(\omega)}{d\omega})$  and  $\text{Im}(\epsilon_{\text{eff}}(\omega))$  when  $\text{Im}(\frac{d\epsilon_{\text{eff}}(\omega)}{d\omega}) = 0$ , the latter being a necessary condition for absorption peak at  $\omega_R$ . Note that the effective permittivity is a function of  $\epsilon_1(\omega)$  and  $\epsilon_2 = 1$ . The derivative with respect to frequency of the effective permittivity can be rewritten as

$$\frac{d\epsilon_{\text{eff}}(\omega)}{d\omega} \Big|_{\omega=\omega_R} = \left( \frac{\partial \epsilon_{\text{eff}}(\epsilon_1(\omega), 1)}{\partial \epsilon_1} \frac{d\epsilon_1(\omega)}{d\omega} \right) \Big|_{\omega=\omega_R}, \quad (3)$$

where  $\frac{d\epsilon_1(\omega)}{d\omega}$  is a known quantity as  $\epsilon_1(\omega)$  is known. This reduces the problem to correlating the quantities  $\partial \epsilon_{\text{eff}}(\epsilon_1(\omega), 1)/\partial \epsilon_1$  and  $\text{Im}(\epsilon_{\text{eff}}(\epsilon_1(\omega), 1))$  at  $\omega = \omega_R$ . To obtain this correlation, we formulate the following problem: Given a fixed realizable value of  $\text{Im}(\epsilon_{\text{eff}}(\epsilon_1(\omega), 1))$  at  $\omega = \omega_R$ , what are the bounds on the values of  $\text{Re}(\partial \epsilon_{\text{eff}}(\epsilon_1(\omega), 1)/\partial \epsilon_1)$ , with the constraint that  $\text{Im}(\frac{\partial \epsilon_{\text{eff}}(\epsilon_1(\omega), 1)}{\partial \omega})|_{\omega=\omega_R} = 0$ , which is associated with absorption peak at  $\omega = \omega_R$ ? We solve this problem numerically by using the bounds of Milton *et al.*<sup>18,22,26,27</sup> (see, Chap. 27 in Milton<sup>27</sup>) (for details, see supplementary material Sec. S2). In fact, in a broader mathematical context outside the theory of composites, there is a long history of such bounds.<sup>28</sup> From the bounds, we then easily obtain constraints on  $Q_{\text{new}}$  for any possible value of  $\text{Im}(\epsilon_{\text{eff}}(\epsilon_1(\omega_R), 1))$ .

First, we present our results with  $\epsilon_1(\omega)$  given by the Drude model,

$$\epsilon_1(\omega) = 1 + \omega_p^2/(\omega^2 + i\omega\gamma) \quad (4)$$

with,  $\omega_p = 5$ ,  $\gamma = 0.1$ . Plots for bounds on the effective complex permittivity  $\epsilon_{\text{eff}}(\omega_R)$  and for the corresponding range of  $d\epsilon_{\text{eff}}/d\omega$  in this

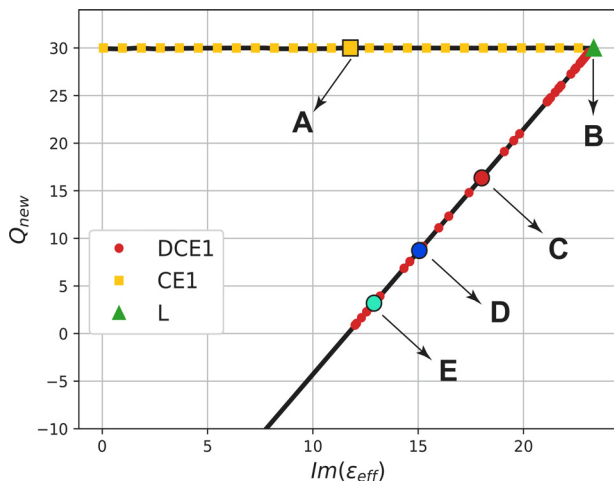


**FIG. 2.**  $Q_{\text{new}}$  vs  $\text{Im}(\epsilon_{\text{eff}})$  for two-phase metamaterial quasi-static absorption peaks with  $\epsilon_1(\omega)$  given by the Drude model. Bounds on  $Q_{\text{new}}$  (solid black curve) are shown as the value of  $\text{Im}(\epsilon_{\text{eff}}(\omega_R))$  at a center frequency of  $\omega_R = 3$  is varied within the range of  $\epsilon_{\text{eff}}(\omega_R)$ . Metamaterial geometries achieving all points on these bounds are shown: Coated ellipsoids (CE1: yellow squares) attain values on the upper bound for  $Q_{\text{new}}$  as the eccentricities and volume fractions of the core phase are varied; laminate geometry (L: green triangle) attains the point on extreme right; points on the lower bound are achieved by doubly coated ellipsoids (DCE1: red circles). Specific points on the bounds are highlighted as A, B, C, D, and E, and more information on the microstructure geometries at these points is given in **Fig. 3**.

case are shown in the supplementary material (Sec. S2). **Figure 2** shows the wedge-shaped bounds on  $Q_{\text{new}}$  (shown by the solid black curve) as the absorption peak value of  $\text{Im}(\epsilon_{\text{eff}})$  varies within the range prescribed by  $\epsilon_{\text{eff}}(\omega_R)$ . Our bounds on  $Q_{\text{new}}$  allow for  $\text{Re}(\text{d}\epsilon_{\text{eff}}(\omega)/\text{d}\omega)$  at  $\omega = \omega_R$  to be positive. From (2), we then see that negative values of  $Q_{\text{new}}$  are allowed by the bounds as in **Fig. 2**. Negative Q-factor values are irrelevant for our study, and as such they must be ignored in our bounds.

Furthermore, we find the optimal metamaterial microstructures that achieve these bounds. Specifically, points on the upper horizontal bound are achieved by assemblages of confocal coated ellipsoids (CE1) with the core phase given by  $\epsilon_1(\omega)$  (4). The effective permittivity of the coated ellipsoid (CE1) has two free parameters:<sup>27</sup> the depolarization factor and the volume fraction. The depolarization factor is used to tune the resonance, and the volume fraction can be varied within limits to trace points on the upper bound. In **Fig. 2**, the yellow square markers denote the values from CE1. Simple laminate geometries (L), with the volume fraction tuned to get absorption peak at the desired frequency, attain only the extreme right point on the bounds (green triangle), when the layers of the laminate are normal to the direction of the electric field. When the electric field is parallel to the layers, the laminate effective permittivity is an arithmetic mean of  $\epsilon_1(\omega)$  and  $\epsilon_2 = 1$ , and consequently, there is no resonance observed at any frequency. The lower bound in **Fig. 2** is traced by assemblages of highly sensitive doubly coated ellipsoids (DCE1, shown by red circles) where the innermost and outermost phases are the same and given by  $\epsilon_1(\omega)$ . The inner coated ellipsoid and outer coated ellipsoid are not restricted to have the same eccentricities and, hence, are more general than confocal doubly coated ellipsoids. Doing so provides us with four

parameters: the depolarization factor of the inner coated ellipsoid, depolarization factor of the outer coated ellipsoid, volume fraction of the Drude phase, and volume fraction of the core phase. These parameters can be varied so that the resulting effective permittivity function  $\epsilon_{\text{eff}}(\epsilon_1, 1)$  matches any formula that defines the bounds (see, Sec. 18.5 in Milton<sup>27</sup>). As such, the assemblages of doubly coated ellipsoids necessarily attain values on the bound.

In **Fig. 3**, we present schematic drawings of the optimal metamaterial designs corresponding to three specific points A, B, and C on the bounds in **Fig. 2**. In each of the subfigures,  $\epsilon_1(\omega)$  is shown in pink color, and the constant phase  $\epsilon_2 = 1$  is shown in gray color. Point A corresponds to a coated ellipsoid assemblage depicted in **Fig. 3(a)**. Point B corresponds to a material with laminate geometry, which is shown in **Fig. 3(b)**. Most interesting is point C that corresponds to a limiting case of doubly coated ellipsoid geometry as described before, with the following parameters: depolarization factors of the inner and outer coated ellipsoid are 0.5614 and 1, respectively, the volume fraction of the outermost phase = 0.4374, and volume fraction of the core phase = 0.000 236 3. Thus, the ellipsoidal inclusions only occupy an extremely small volume fraction, but are significant due to resonance effects. The schematic drawing seen in **Fig. 3(c)** depicts this laminate geometry, common to the points C, D, and E, with the constant phase (outermost layer of DCE1) forming one of the laminates, and the second laminate being formed from a very dilute assemblage of coated ellipsoids (inner coated ellipsoid of DCE1).

For each microgeometry,  $Q_{\text{new}}$  values attaining the bounds are obtained when the electric field is applied in the direction of the blue arrows.

Next, we obtain the response of  $\epsilon_{\text{eff}}(\omega)$  with respect to  $\omega$  for the specific geometries indicated by the points A (CE1), B (L), C (DCE1), D (DCE1), and E (DCE1) in **Fig. 2**. **Figures 4(a)** and **4(b)** show the plots for  $\text{Im}(\epsilon_{\text{eff}})$  vs  $\omega$  and  $\text{Re}(\epsilon_{\text{eff}})$  vs  $\omega$ , respectively, for three

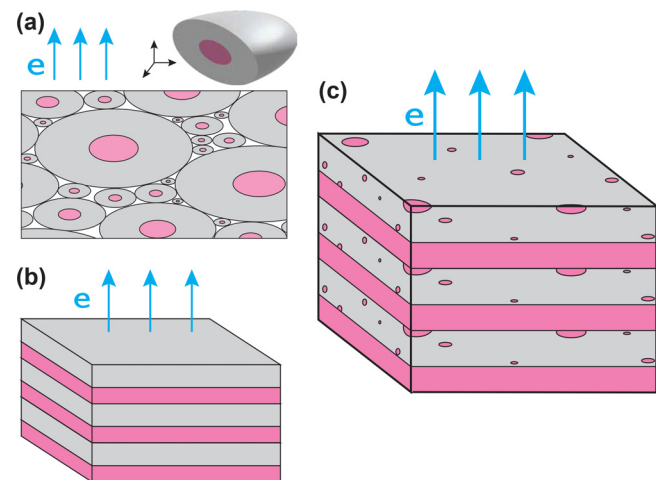


**FIG. 3.** Optimal two-phase metamaterial microstructure designs: The pure phase with permittivity given by the Drude model is shown in pink, and the pure phase with constant permittivity is shown in gray. (a) Coated ellipsoid (CE1) assemblage corresponding to point A in **Fig. 2**. (b) Laminate geometry (L), corresponding to point B in **Fig. 2**. (c) Doubly coated ellipsoid (DCE1) assemblage (points C, D, and E in **Fig. 2**). In each of the designs, the optimal  $Q_{\text{new}}$  is obtained in the direction of the applied electric field (seen in blue).

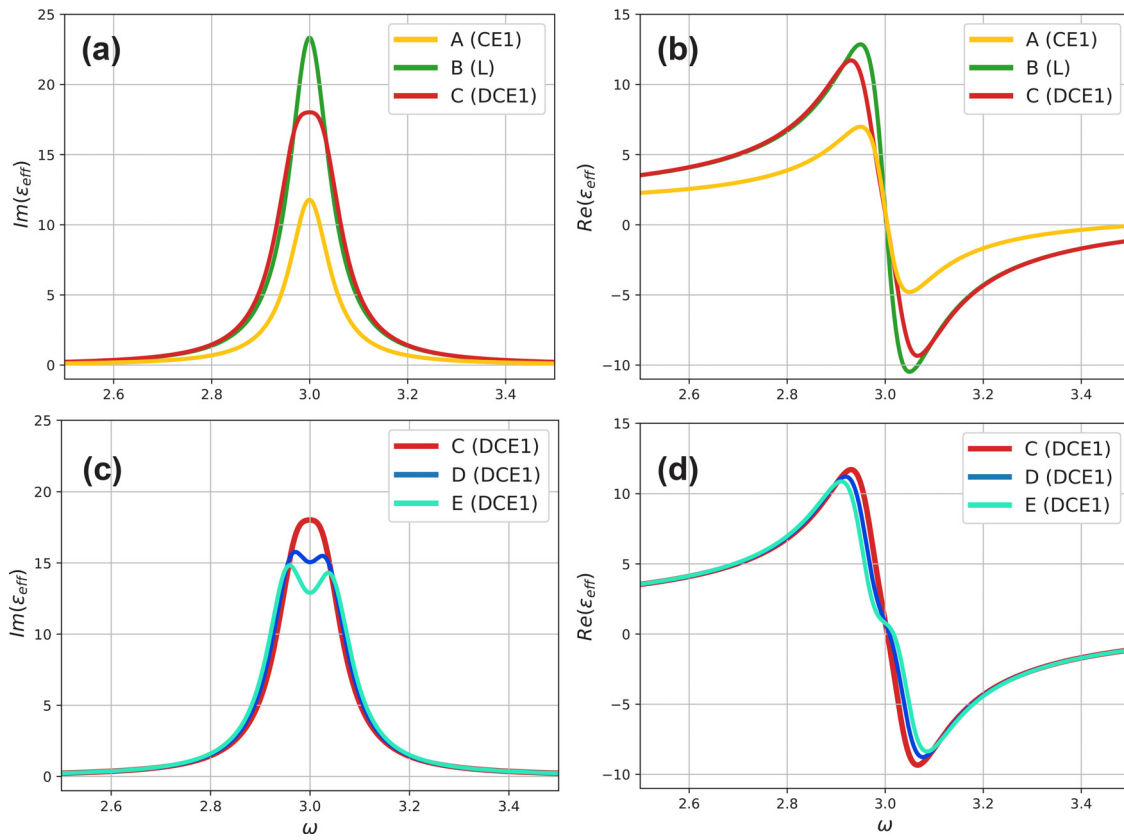


**FIG. 4.** Plots of  $\epsilon_{\text{eff}}$  vs  $\omega$ , associated with the optimal metamaterial designs. (a)  $\text{Im}(\epsilon_{\text{eff}})$  vs  $\omega$ , and (b)  $\text{Re}(\epsilon_{\text{eff}})$  vs  $\omega$ , for the points A (coated ellipsoid, CE1, shown here by yellow line), B (laminate, L, shown by green line), and C (doubly coated ellipsoid, DCE1, shown by red line) from Fig. 2. (c) and (d) Plots for  $\text{Im}(\epsilon_{\text{eff}})$  vs  $\omega$ , and  $\text{Re}(\epsilon_{\text{eff}})$  vs  $\omega$ , respectively, for three different doubly coated ellipsoid geometries that achieve the points C, D, and E on the bounds in Fig. 2. Note that the behavior of  $\text{Im}(\epsilon_{\text{eff}})$  in (c), where we can see a small local minimum for D and E (blue and cyan colored curves, respectively) at  $\omega_R = 3$ . For these cases, the value of  $\text{Im}(\epsilon_{\text{eff}})$  at the center frequency is not quite the overall peak height.

16 March 2024 12:03:51

different geometries given by points A, B, and C. Despite the large difference in the  $\text{Im}(\epsilon_{\text{eff}})$  values of points A (CE1, seen in yellow) and B (L, seen in green), they have the same  $Q_{\text{new}}$ . Figures 4(c) and 4(d) show a similar comparison, but for three similar doubly coated ellipsoid geometries that attain points C, D, and E on the lower bound. Interestingly, we observe that as we move from point C toward point E, the values of  $\text{Im}(\epsilon_{\text{eff}})$  at center frequency undergo a transition and exhibit a small local minimum at the center frequency of the bandwidth [shown by blue and cyan colored curves in Fig. 4(c)]. This, and even the peak in C, is due to two resonances contributing to the peak. If one wishes to only consider peaks without such local minima, we could improve the bounds by adding the additional constraint that  $d^2\text{Im}(\epsilon_{\text{eff}})/d\omega^2 \leq 0$ . This can be done but would further complicate the analysis.

Similarly, bounds on  $Q_{\text{new}}$  can be obtained for the case when the permittivity of the pure phase  $\epsilon_1(\omega)$  is given by a Lorentz model. In the supplementary material Sec. S3, we present plots for  $Q_{\text{new}}$  vs  $\text{Im}(\epsilon_{\text{eff}})$  for three different frequencies: one, at the resonance frequency of the pure phase; two, near the resonance of the pure phase; and, three, at a frequency away from the resonance of the pure phase. These results show that the region enclosed by the  $Q_{\text{new}}$  bounds can be non-convex.

We now obtain bounds on  $Q_{\text{new}}$ , when the two-phase metamaterials are three-dimensional (3D), isotropic, and have fixed volume fraction  $f_1$  for the pure phase  $\epsilon_1(\omega)$ , given by the Drude model, and  $\epsilon_2 = 1$ . To obtain bounds including the volume fraction and isotropy of the microstructure, we let  $f_2 = 1 - f_1$ , be the volume fraction of phase 2, and introduce the function,<sup>29</sup>

$$\epsilon_{\text{eff}}(\epsilon_1, \epsilon_2) = -\frac{1}{2}f_2\epsilon_1 - \frac{1}{2}f_1\epsilon_2 + \frac{f_1f_2(\epsilon_1 - \epsilon_2)^2}{2[f_1\epsilon_1 + f_2\epsilon_2 - \epsilon_{\text{eff}}]}, \quad (5)$$

(related to the so-called Y transform;<sup>22</sup> see, Chaps. 19 and 20 in Ref. 27) that has basically the same analytic properties and, hence, is subject to basically the same bounds, as  $\epsilon_{\text{eff}}(\epsilon_1, \epsilon_2)$ . In the case of metal particle clusters with overall isotropic polarizability  $\alpha$ , (5) reduces to

$$\tilde{\epsilon}_{\text{eff}}(\epsilon_1, \epsilon_2) = -\frac{1}{2}\epsilon_1 + \frac{(\epsilon_1 - \epsilon_2)^2}{2[(\epsilon_1 - \epsilon_2) - \alpha/V]}, \quad (6)$$

where  $V$  is the volume of the particle clusters. Thus, for example,  $\tilde{\epsilon}_{\text{eff}} = \epsilon_2$  for a sphere with polarizability  $\alpha = 3V\epsilon_2(\epsilon_1 - \epsilon_2)/(\epsilon_1 + 2\epsilon_2)$ . In the isotropic case, bounds on  $\epsilon_{\text{eff}}$  with known volume fraction were first obtained by Bergman and Milton<sup>18,22,26,30</sup> and were

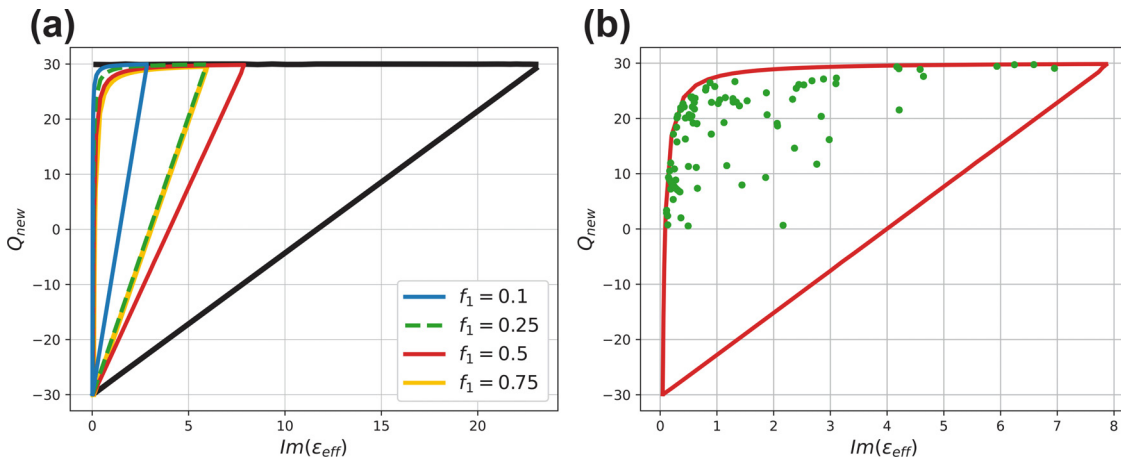


**FIG. 5.** Bounds on  $Q_{\text{new}}$  for 3D, isotropic, and fixed volume fraction two-phase quasi-static metamaterial resonators at the center frequency  $\omega_R = 3$  with  $\epsilon_1(\omega)$  given by the Drude model. (a)  $Q_{\text{new}}$  bounds for volume fractions  $f_1 = 0.1$  (blue line),  $f_1 = 0.25$  (dashed green line),  $f_1 = 0.5$  (red line),  $f_1 = 0.75$  (yellow line) are superposed for comparison with the volume fraction independent bounds (solid black curve). (b)  $Q_{\text{new}}$  values obtained from Schulgasser laminates of doubly coated ellipsoids with the outer coated ellipsoid forming a prolate spheroid are plotted (green circles). The solid red line in (b) denotes the bounds for  $f_1 = 0.5$ . Some of the doubly coated ellipsoid geometries are found to be almost optimal.

recently improved by Kern *et al.*<sup>31</sup> We seek bounds that also involve  $\frac{d\epsilon_{\text{eff}}(\omega)}{d\omega}$  (see supplementary material Sec. S4 for more explanation).

Bounds on  $Q_{\text{new}}$  for all possible values of  $\text{Im}(\epsilon_{\text{eff}})$  are obtained for four different volume fractions,  $f_1 = 0.1, 0.25, 0.5$ , and  $0.75$ , for a center frequency of  $\omega_R = 3$ . Figure 5(a) shows all the 3D, isotropic, fixed volume fraction bounds superposed on top of the bounds shown in Fig. 2 for comparison, as they are all evaluated at the same frequency  $\omega_R = 3$ . The plots show that the area of the region occupied by the bounds does not monotonically increase as the volume fraction is increased, which is clear since the bounds for  $f_1 = 0.5$  (solid red curve) occupies a larger region than the bounds for  $f_1 = 0.75$  (solid yellow curve), and the bounds for  $f_1 = 0.25$  (dashed green curve). Not surprisingly, the bounds at fixed volume fraction correlating  $Q_{\text{new}}$  with  $\text{Im}(\alpha)$ , when  $\text{Im}(\frac{d\alpha(\omega)}{d\omega}) = 0$ , are qualitatively similar to those correlating  $Q_{\text{new}}$  with  $\text{Im}(\epsilon_{\text{eff}})$ , when  $\text{Im}(\frac{d\epsilon_{\text{eff}}(\omega)}{d\omega}) = 0$  as in Fig. 5(b). For this reason, the polarizability bounds are presented in the supplementary material rather than here.

Here too, we find some optimal isotropic, fixed volume fraction metamaterial designs that attain certain points on the bounds by using the Schulgasser<sup>32</sup> lamination technique to construct the isotropic effective permittivities. Given an anisotropic effective tensor  $\epsilon_{\text{eff}}$ , he showed that one could obtain an isotropic material with permittivity  $\text{Tr}(\epsilon_{\text{eff}})/3$ .

The almost optimal geometries are Schulgasser laminates of assemblages of doubly coated ellipsoids with the outer coated ellipsoid forming a prolate spheroid, while there is no special form of the inner coated ellipsoid (see the supplementary material for parameter values). Figure 5(b) shows the  $Q_{\text{new}}$  values (green dots) obtained by doubly coated ellipsoids with outer coated ellipsoid taken to be prolate spheroids for a volume fraction of  $f_1 = 0.5$ , with some microstructures apparently attaining points on the bound.

Similarly, bounds on  $Q_{\text{new}}$  can be obtained for 3D, isotropic, fixed volume fraction materials using the Lorentz model for  $\epsilon_1(\omega)$ . The associated results are presented in the supplementary material, Fig. 8. Note that, when phase 1 is Lorentzian,  $\epsilon_{\text{eff}}$  may have absorption peaks

due to both resonance of the pure Lorentzian phase and resonances due to the composite microgeometry. Instead, if the phase 1 is given by the Drude model (4) and  $\epsilon_2 = 1$ , then  $\epsilon_{\text{eff}}$  has absorption peaks due to microstructure geometry only.

In conclusion, our work provides bounds in quasi-statics correlating a newly defined Q-factor with the peak absorption in two-phase composites and clusters of particles. It allows for peaks generated by more than one resonance. Such peaks are important in nano-photonics and optics. Optimal metamaterial microstructures have been identified that achieve these limits. It will be interesting to see how these theoretical and numerical results compare against any experiments in the quasi-static regime or invalidate them at higher frequencies.

See the supplementary material for additional details related to this work.

The authors are grateful to the National Science Foundation for support through Grant No. DMS-2107926. We thank Mats Gustafsson for suggesting a connection between Q-factor and the derivative  $\text{Re}(\frac{d\epsilon_{\text{eff}}(\omega)}{d\omega})$  at absorption peak. This formed the basis for our formula for  $Q_{\text{new}}$ . We are very grateful to the reviewers who provided helpful comments that led to significant improvements in the paper.

## AUTHOR DECLARATIONS

### Conflict of Interest

The authors have no conflicts to disclose.

### Author Contributions

K. J. Deshmukh and G. W. Milton contributed equally on this paper.

**Kshiteej Jayendra Deshmukh:** Conceptualization (equal); Formal analysis (equal); Investigation (equal); Validation (equal); Writing –

original draft (equal); Writing – review & editing (equal). **Graeme Milton:** Conceptualization (equal); Formal analysis (equal); Funding acquisition (lead); Investigation (equal); Validation (equal); Writing – original draft (equal); Writing – review & editing (equal).

## DATA AVAILABILITY

The data that support the findings of this study are available within the article and its supplementary material.

## REFERENCES

- <sup>1</sup>S. A. Maier and H. A. Atwater, "Plasmonics: Localization and guiding of electromagnetic energy in metal/dielectric structures," *J. Appl. Phys.* **98**, 011101 (2005).
- <sup>2</sup>F. Wang and Y. R. Shen, "General properties of local plasmons in metal nanostructures," *Phys. Rev. Lett.* **97**, 206806 (2006).
- <sup>3</sup>R. Collin and S. Rothschild, "Evaluation of antenna Q," *IEEE Trans. Antennas Propag.* **12**, 23–27 (1964).
- <sup>4</sup>R. Fante, "Quality factor of general ideal antennas," *IEEE Trans. Antennas Propag.* **17**, 151–155 (1969).
- <sup>5</sup>D. R. Rhodes, "Observable stored energies of electromagnetic systems," *J. Franklin Inst.* **302**, 225–237 (1976).
- <sup>6</sup>A. D. Yaghjian and S. R. Best, "Impedance, bandwidth, and Q of antennas," *IEEE Trans. Antennas Propag.* **53**, 1298–1324 (2005).
- <sup>7</sup>M. Gustafsson and S. Nordebo, "Bandwidth, Q factor, and resonance models of antennas," *Prog. Electromagn. Res.* **62**, 1–20 (2006).
- <sup>8</sup>A. Figotin and A. Welters, "Dissipative properties of systems composed of high-loss and lossless components," *J. Math. Phys.* **53**, 123508 (2012).
- <sup>9</sup>L. J. Chu, "Physical limitations of omni-directional antennas," *J. Appl. Phys.* **19**, 1163–1175 (1948).
- <sup>10</sup>H. R. Stuart, "Bandwidth limitations in small antennas composed of negative permittivity materials and metamaterials," in XXIX General Assembly of the International Union of Radio Science (URSI), Chicago, IL, 2008.
- <sup>11</sup>A. D. Yaghjian and H. R. Stuart, "Lower bounds on the Q of electrically small dipole antennas," *IEEE Trans. Antennas Propag.* **58**, 3114–3121 (2010).
- <sup>12</sup>M. Gustafsson and S. Nordebo, "Optimal antenna currents for Q, superdirective, and radiation patterns using convex optimization," *IEEE Trans. Antennas Propag.* **61**, 1109–1118 (2013).
- <sup>13</sup>M. Gustafsson, M. Cismasu, and B. L. G. Jonsson, "Physical bounds and optimal currents on antennas," *IEEE Trans. Antennas Propag.* **60**, 2672–2681 (2012).
- <sup>14</sup>M. Gustafsson, D. Tayli, M. Cismasu, and Z. Chen, "Physical bounds of antennas," in *Handbook of Antenna Technologies* (Springer, Singapore, 2015).
- <sup>15</sup>B. L. G. Jonsson and M. Gustafsson, "Stored energies in electric and magnetic current densities for small antennas," *Proc. R. Soc. A* **471**, 20140897 (2015).
- <sup>16</sup>M. Pascale, S. A. Mann, D. C. Tzarouchis, G. Miano, A. Alù, and C. Forestiere, "Lower bounds to the Q factor of electrically small resonators through quasi-static modal expansion," *IEEE Trans. Antennas Propag.* **71**, 4350 (2023).
- <sup>17</sup>D. J. Bergman, "The dielectric constant of a composite material—A problem in classical physics," *Phys. Rep.* **43**, 377–407 (1978).
- <sup>18</sup>G. W. Milton, "Bounds on the complex dielectric constant of a composite material," *Appl. Phys. Lett.* **37**, 300–302 (1980).
- <sup>19</sup>O. D. Miller, C. W. Hsu, M. T. H. Reid, W. Qiu, B. G. DeLacy, J. D. Ioannopoulos, M. Soljačić, and S. G. Johnson, "Fundamental limits to extinction by metallic nanoparticles," *Phys. Rev. Lett.* **112**, 123903 (2014).
- <sup>20</sup>G. W. Milton, R. C. McPhedran, and D. R. McKenzie, "Transport properties of arrays of intersecting cylinders," *Appl. Phys.* **25**, 23–30 (1981).
- <sup>21</sup>G. W. Milton, "Bounds on complex polarizabilities and a new perspective on scattering by a lossy inclusion," *Phys. Rev. B* **96**, 104206 (2017).
- <sup>22</sup>G. W. Milton, "Bounds on the complex permittivity of a two-component composite material," *J. Appl. Phys.* **52**, 5286–5293 (1981).
- <sup>23</sup>M. Gustafsson and B. L. G. Jonsson, "Stored electromagnetic energy and antenna Q," *Prog. Electromagn. Res.* **150**, 13–27 (2015).
- <sup>24</sup>K. Schab, L. Jelinek, M. Capek, C. Ehrenborg, D. Tayli, G. A. Vandenbosch, and M. Gustafsson, "Energy stored by radiating systems," *IEEE Access* **6**, 10553–10568 (2018).
- <sup>25</sup>A. Welters, Y. Avniel, and S. G. Johnson, "Speed-of-light limitations in passive linear media," *Phys. Rev. A* **90**, 023847 (2014).
- <sup>26</sup>G. W. Milton, "Bounds on the transport and optical properties of a two-component composite material," *J. Appl. Phys.* **52**, 5294–5304 (1981).
- <sup>27</sup>G. W. Milton, *The Theory of Composites* (Society for Industrial and Applied Mathematics, Philadelphia, PA, 2022).
- <sup>28</sup>M. G. Krein and A. A. Nudelman, *Translations of Mathematical Monographs* (AMS, 1977) Vol. 50, pp. 417.
- <sup>29</sup>G. Milton and K. Golden, "Thermal conduction in composites," in *Thermal Conductivity*, edited by T. Ashworth and D. R. Smith (Springer, Boston, MA, 1985).
- <sup>30</sup>D. J. Bergman, "Exactly solvable microscopic geometries and rigorous bounds for the complex dielectric constant of a two-component composite material," *Phys. Rev. Lett.* **45**, 148–148 (1980).
- <sup>31</sup>C. Kern, O. D. Miller, and G. W. Milton, "Tight bounds on the effective complex permittivity of isotropic composites and related problems," *Phys. Rev. Appl.* **14**, 054068 (2020).
- <sup>32</sup>K. Schulgasser, "Bounds on the conductivity of statistically isotropic polycrystals," *J. Phys. C* **10**, 407 (1977).